

# On the Prospects of Measuring the Cosmic Dawn 21-cm Power Spectrum using the Upgraded Giant Meterwave Radio Telescope (uGMRT)

Suman Chatterjee<sup>1,2\*</sup>, Somnath Bharadwaj<sup>1,2†</sup>

<sup>1</sup>*Department of Physics, Indian Institute of Technology Kharagpur, Kharagpur - 721 302, India.*

<sup>2</sup>*Centre for Theoretical Studies, Indian Institute of Technology Kharagpur, Kharagpur - 721 302, India.*

11 December 2018

## ABSTRACT

A recent observation by the EDGES collaboration shows a strong absorption signal in the global 21-cm spectrum from around a redshift of  $z = 17$ . This absorption is stronger than the maximum prediction by existing models and indicates that the spatial fluctuations of the HI 21-cm brightness temperature at Cosmic Dawn could be an order of magnitude larger than previously expected. In this paper, we investigate the prospects of detecting the HI 21-cm power spectrum from Cosmic Dawn using uGMRT. We find that a  $10\sigma$  detection of the enhanced HI 21-cm signal power spectrum is possible within 70, 140 and 400 Hours of observation for an optimistic, moderate and pessimistic scenario respectively, using the Band-1 of uGMRT. This could be an useful probe of the interaction between the baryon and dark matter particles in the early universe. We also present a comparison of the uGMRT predictions with those for the future SKA-Low.

**Key words:** Interferometric; cosmology: observations, Cosmic Dawn, large-scale structure of Universe

## 1 INTRODUCTION

Observations with the Experiment to Detect the Global Epoch of Reionization Signature (EDGES) have recently resulted in the detection of an absorption profile with full width half maxima (FWHM) 19 MHz centred at 78 MHz in the sky averaged spectrum of the background radiation in the frequency range 50 – 100 MHz (Bowman et al. 2018). If confirmed by other similar experiments like the Large-Aperture Experiment to Detect the Dark Ages (LEDA; Bernardi et al. 2016), the Sonda Cosmológica de las Islas para la Detección de Hidrógeno Neutro (SCI-HI; Voytek et al. 2014), the Probing Radio Intensity at high  $z$  from Marion (PRIZM; Philip et al. 2018) and the Shaped Antenna measurement of the background Radio Spectrum 2 (SARAS 2; Singh et al. 2017), this can be interpreted as the neutral Hydrogen (HI) 21-cm absorption profile resulting from the Lyman- $\alpha$  coupling due to the formation of the first stars in the early universe (Pritchard & Loeb 2012). However, the observation indicates a dip with amplitude 0.5 K which is more than a factor of two larger than the largest predictions (Cohen et al. 2017). Barkana (2018) have proposed that it is possible to explain this enhanced dip through a

possible interaction between the baryons and dark matter particles (b-DM interaction). Such models (Barkana 2018; Fialkov et al. 2018) have predicted a 10 fold enhancement of the spatial fluctuations of the redshifted HI 21-cm brightness temperature  $\delta T_b(x)$ . We note that other alternative explanations have also been proposed (Ewall-Wice et al. 2018; Feng & Holder 2018) to explain the enhanced dip. The latter models incorporate an enhancement in the radio background and they do not predict such enhancement in  $\delta T_b(x)$ .

Dvorkin et al. (2014), Tashiro et al. (2014), Muñoz et al. (2015) and Xu et al. (2018) have considered b-DM interaction in the context of cosmology and large-scale structure formation. Barkana (2018) have assumed a non-standard Coulomb-like interaction between dark-matter particles and baryons that does not depend on whether the baryons are free or bound within atoms. By combining this with the radiation emitted by the first stars during cosmic dawn, they find a strong 21-cm absorption that can explain the feature measured by EDGES. These models (Barkana 2018; Fialkov et al. 2018) also predict a 10 fold enhancement of the spatial fluctuations of the redshifted HI 21-cm brightness temperature  $\delta T_b(x)$ . Muñoz & Loeb (2018) explore whether dark-matter particles with an electric “minicharge” can significantly alter the baryonic temperature and affect the global 21-cm signal. They find that the entire dark matter cannot be minicharged at a significant level, the constraints

\* E-mail: suman05@phy.iitkgp.ernet.in

† E-mail: somnath@phy.iitkgp.ernet.in

coming from Galactic and extragalactic magnetic fields. However, minicharged particles that comprise a subpercent fraction of the dark matter and have a charge  $\sim 10^{-6}$  in units of the electron charge and masses  $m_\chi \sim 1 - 60$  MeV can significantly cool down the baryons and explain the EDGES result while remaining consistent with other observational constraints. In a recent paper, subsequent to the submission of the present *paper*, [Muñoz et al. \(2018\)](#) have analysed the 21-cm brightness temperature fluctuations for the minicharge model. Their study confirms a significant enhancement in the predicted 21-cm brightness temperature fluctuations, including an increase in the amplitude of the baryon acoustic oscillation.

Upcoming experiments such as the Hydrogen Epoch of Reionization Array (HERA; [DeBoer et al. 2017](#)) and the Square Kilometre Array (SKA; [Koopmans et al. 2015](#)) have the potential of measuring the HI 21-cm power spectrum from Cosmic Dawn (50 – 100 MHz). Both of these experiments should easily be able to measure the corresponding enhanced HI 21-cm power spectrum predicted by the b-DM interaction models ([Barkana 2018](#)).

The Giant Meterwave Radio Telescope (GMRT; [Swarup et al. 1991](#)) is one of the largest and most sensitive fully operational low-frequency radio telescopes in the world today. The array configuration of 30 antennas (each of 45 m diameter) spanning over 25 km, provides a total collecting area of about 30,000 sq. m at metre wavelengths. The GMRT is being upgraded (uGMRT, [Gupta et al. 2017](#)) to have seamless frequency coverage, as far as possible, from 50 to 1500 MHz. Band-1 of uGMRT, which is yet to be implemented, is expected to cover the frequency range 50 – 80 MHz. Earlier [Shankar et al. \(2009\)](#) envisaged a 50 MHz system developed for GMRT to provide imaging capability in the frequency range 30 – 90 MHz.

In this paper, we investigate the prospects of detecting the redshifted HI 21-cm signal power spectrum from Cosmic Dawn using the uGMRT. For the purpose of this analysis we have considered a functional bandwidth of  $B = 20$  MHz centred at  $\nu_c = 78$  MHz, consistent with the frequency coverage described in [Shankar et al. \(2009\)](#). Frequencies above 90 MHz are used for FM transmission which restricts the allowed frequency range. We have also carried out a similar analysis for the future SKA-Low, and we present a comparison of the predictions for the uGMRT with those for the future SKA-Low.

## 2 METHODOLOGY

We have simulated the uGMRT baseline configuration for 8 hours of observation targeted on a field at  $+60^\circ$  DEC with 16 s integration time. The entire analysis has been restricted to baselines with antenna separations within 2 km, which contains the bulk of the cosmological signal. We assume that the bandwidth  $B = 20$  MHz is divided into  $N_c = 200$  spectral channels of  $\Delta\nu_c = 100$  KHz. Note that the values of  $B$ ,  $N_c$  and  $\Delta\nu_c$  assumed here are only representative values, and the actual values in the final implementation of the telescope may be somewhat different. The 20 MHz bandwidth spans the redshift range  $z = 15$  to 20, and the HI 21-cm power spectrum may evolve significantly within this redshift range. Consequently we have considered three bands each of width

6 MHz centred at 72 MHz, 78 MHz and 84 MHz which correspond to  $z = 18.7, 17.2$  and  $15.9$  respectively. We assume that the measurements from these three bands are combined to enhance the signal-to-noise ratio (SNR).

Considering the simulated baseline  $u - v$  distribution, we use  $\mathbf{k}_\perp = 2\pi\mathbf{U}/r$  and  $k_{\parallel m} = 2\pi m/r'B$  to estimate the Fourier modes at which the brightness temperature fluctuations  $\Delta T(\mathbf{k})$  will be measured by this observation. Here  $\mathbf{U}$  refer to different baselines,  $0 \leq m \leq N_c/2$ ,  $r$  is the co-moving distance corresponding to  $\nu_c$  and  $r' = dr/d\nu$  evaluated at  $\nu = \nu_c$ . We assume that the measured  $\Delta T(\mathbf{k})$  values are gridded in  $(\mathbf{k}_\perp, k_{\parallel})$  space with a grid spacing  $\Delta k_\perp = 2\pi D/\lambda_c r$  and  $\Delta k_{\parallel} = 2\pi/r'B$ , and the gridded values are used to estimate the power spectrum  $P(\mathbf{k}_g)$  at each grid point  $\mathbf{k}_g$ . Here we have used the simulation to estimate the sampling function  $\tau(\mathbf{k}_g)$  which refers to the number of distinct  $\Delta T(\mathbf{k})$  measurements that contribute to each grid point  $\mathbf{k}_g$ .

For the Cosmic Dawn HI 21-cm signal we have used the value of the dimensionless HI 21-cm power spectrum  $\Delta_{\text{HI}}^2(k) = k^3 P_{\text{HI}}(k)/2\pi^2$  from earlier works ([Santos et al. 2010](#); [Mellema et al. 2013](#)), where  $P_{\text{HI}}(k)$  refers to the HI 21-cm power spectrum. ([Barkana 2018](#); [Fialkov et al. 2018](#)). We have used the  $z = 17$  HI 21-cm power spectrum predictions from [Santos et al. \(2010\)](#) as the fiducial model for all the three bands which we have considered here. These values correspond to the standard scenario, we expect a 10 fold enhancement in the brightness temperature fluctuations *i.e.* a dimensionless power spectrum of  $100\Delta_{\text{HI}}^2$  in the presence of the b-DM interaction

In addition to the HI 21-cm power spectrum, we also have the noise power spectrum  $P_N(\mathbf{k}_\perp, k_{\parallel})$  which can be estimated as follows. The measured power spectrum is related to the observed visibilities  $V(\mathbf{U}, \nu)$  as

$$P(\mathbf{k}_\perp, k_{\parallel}) = \frac{r'}{\tilde{Q}} \int \langle V(\mathbf{U}, \nu) V^*(\mathbf{U}, \nu + \Delta\nu) \rangle d(\Delta\nu) \quad (1)$$

which can be obtained from (eq. 15.) of [Bharadwaj & Ali \(2005\)](#), where  $\tilde{Q} = (\partial B/\partial T)^2 r^{-2} \int A(\theta)^2 d^2\theta$ ,  $A(\theta)$  is the primary beam pattern of the telescope,  $(\partial B/\partial T) = 2k_B/\lambda^2$ , Considering the noise contribution  $N(\mathbf{U}, \nu)$  to the observed visibilities  $V(\mathbf{U}, \nu)$ , and assuming that the noise at two different frequency channels is uncorrelated, we have the noise power spectrum contribution from the visibilities measured at a single baseline  $\mathbf{U}$  to be

$$P_N(\mathbf{k}_\perp, k_{\parallel}) = \frac{r' \langle |N(\mathbf{U}, \nu)|^2 \rangle \Delta\nu_c}{\tilde{Q}} \quad (2)$$

which is independent of  $k_{\parallel}$ . The real and imaginary parts of  $N(\mathbf{U}, \nu)$  both have equal variance  $\sigma_N^2$  ([Chengalur et al. 2007](#)) with

$$\sigma_N^2 = \frac{2}{N_p \Delta\nu_c \Delta t} \left( \frac{k_B T_{sys}}{\eta A_g} \right)^2 \quad (3)$$

where  $T_{sys}$  is the system temperature,  $\Delta t$  is the integration time,  $N_p$  is the number of polarizations and the antenna efficiency  $\eta$  is defined through  $\lambda^2/\eta A_g = \int A(\theta) d^2\theta$  where  $A_g$  is the geometrical area of the antennas.

In our analysis we have gridded the simulated baseline distribution on to the  $(\mathbf{k}_\perp, k_{\parallel})$  grid introduced earlier. Figure 5 of [Choudhuri et al. 2014](#) shows the baseline distribution corresponding to the uGMRT observations considered

here. Note that the  $U$  values need to be multiplied by a factor of  $\approx 2$  to scale them from 150 MHz (Choudhuri et al. 2014) to the central frequency 78 MHz considered here. We see that the simulated baselines do not uniformly sample the  $u-v$  (or equivalently  $\mathbf{k}_\perp$ ) plane, and we have used the grid sampling function  $\tau(\mathbf{k}_g)$  to quantify the number of baselines which contribute to each grid point  $\mathbf{k}_g$ . Incorporating this, the noise power spectrum at each grid point can be expressed as

$$P_N(\mathbf{k}_g) = \frac{T_{sys}^2 r' r^2}{\Delta t N_p \tilde{\eta} \tau(\mathbf{k}_g)}, \quad (4)$$

where we have defined the dimensionless factor  $\tilde{\eta} = [\int A^2(\theta) d^2\theta] / [\int A(\theta) d^2\theta]^2$ .

We have assumed the system temperature  $T_{sys} = 3000$  K, number of polarizations  $N_p = 2$  and integration time  $\Delta t = 16$  s. At the frequencies of our interest the uGMRT primary beam pattern is well approximated by a Gaussian  $A(\theta) = e^{-(\theta/\theta_0)^2}$  with  $\theta_0 = 3.1^\circ$  whereby  $\tilde{\eta} = 54.4$ . Note that it is well justified to use the flat sky approximation for the uGMRT. The analysis till now considers 8 hours of observation which roughly corresponds to a single night. For longer observations, the noise power spectrum has been scaled inversely with the number of observing nights.

We have binned the  $k$ -range accessible to uGMRT into 10 logarithmic bins. For each bin  $a$ , we the binned power spectrum  $P_a = \sum_g w_g P(\mathbf{k}_g)$  is a weighted sum of the power spectrum measured at all the grid points within the bin. The weights have been chosen as  $w_g = AP_{\text{HI}}(\mathbf{k}_g) / [P_{\text{HI}}(\mathbf{k}_g) + P_N(\mathbf{k}_g)]^2$  (with normalization constant  $A$ ) to optimise the SNR. We use the variance  $(\Delta P_a)^2 = 1 / \sum_g [P_{\text{HI}}(\mathbf{k}_g) + P_N(\mathbf{k}_g)]^{-2}$  to quantify the uncertainty with which it will be possible to measure power spectrum in each bin.

Foreground removal (e.g. Ali et al. 2008) is an important issue for detecting the cosmological 21-cm power spectrum. Several studies have shown that the foregrounds are expected to be confined to a wedge which is approximately bounded by

$$k_\parallel \leq \left[ \frac{r \sin(\theta_l)}{r \nu_c} \right] k_\perp \quad (5)$$

in the  $(k_\parallel, k_\perp)$  plane (Datta et al. 2010; Vedantham et al. 2012; Morales et al. 2012; Parsons et al. 2012; Trott et al. 2012) where  $\theta_l$  refers to the largest angle (relative to the telescope's pointing direction) from which we have a significant foreground contamination. Only the  $k$ -modes outside this ‘‘foreground wedge’’ can be used for power spectrum estimation. The exact extent of this wedge is however still debatable (see Pober et al. 2014 for a detailed discussion), and for the purpose of this work we consider three different cases which differ in the extent of the foreground wedge.

- **Case I:** This is the most optimistic scenario, where we assume that the foregrounds have been removed perfectly and the whole  $\mathbf{k}$  space accessible by uGMRT is available for measuring the HI 21-cm signal.

- **Case II:** In this moderate scenario we assume that the foreground contributions from angles beyond  $\theta_l = 18^\circ$  from the center of the field of view are highly suppressed by tapering the sky response (Choudhuri et al. 2014). Note that the first null of the uGMRT primary beam pattern at

78 MHz is expected at  $\sim 6^\circ$ . In this case the Fourier modes  $k_\parallel \leq 1.813 |k_\perp|$  are foreground contaminated (eq. 5), and only the modes outside this foreground wedge are used for measuring the HI 21-cm signal.

- **Case III:** In this pessimistic scenario we assume that the foreground contribution extends till the horizon ( $\theta_l = 90^\circ$ ), and the Fourier modes  $k_\parallel \leq 5.964 |k_\perp|$  are foreground contaminated (eq.5). Only the modes outside this foreground wedge are used for measuring the HI 21-cm signal.

### 3 RESULT

We first consider very large observing times for which  $P_N \rightarrow 0$ , and the  $1 - \sigma$  error  $\Delta P_a$  on the measurement of  $P_a$  converges to the cosmic variance. We find that  $\text{SNR} > 5$  can be achieved at  $k > 0.02 \text{Mpc}^{-1}$ ,  $0.04 \text{Mpc}^{-1}$  and  $0.1 \text{Mpc}^{-1}$  for Case I, Case II and Case III respectively. We only consider these  $k$ -modes for our subsequent analysis. We see that in all the three cases there is a reasonably large  $k$ -range where a detection is possible provided we have sufficiently deep observations.

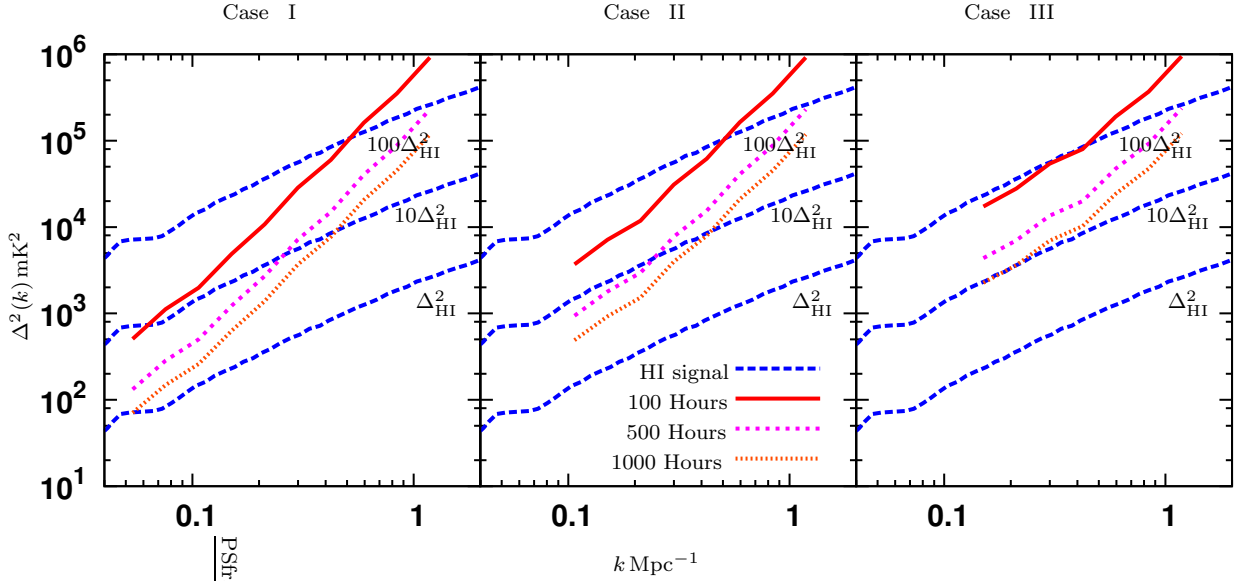
The system noise dominates  $\Delta P_a$  for small observing times. Figure 1 shows a comparison between the dimensionless HI 21-cm signal power spectrum and the corresponding  $1 - \sigma$  error. For Case I we find that  $100\Delta_{\text{HI}}^2$  and  $10\Delta_{\text{HI}}^2$  can be detected with 100 and 500 hours of observation for Fourier modes  $0.06 < k < 0.5 \text{Mpc}^{-1}$  and  $0.06 < k < 0.25 \text{Mpc}^{-1}$  respectively. However, a detection of  $\Delta_{\text{HI}}^2$  will require more than 1000 hours of observation. In Case II, it is possible to detect  $100\Delta_{\text{HI}}^2$  and  $10\Delta_{\text{HI}}^2$  in the  $k$ -range,  $0.1 < k < 0.45 \text{Mpc}^{-1}$  and  $0.1 < k < 0.25 \text{Mpc}^{-1}$  in 100 and 500 hours of observation respectively. For the pessimistic scenario, *i.e.* Case III, we find that  $100\Delta_{\text{HI}}^2$  can be detected in 100 hours of observation in the  $k$ -range  $0.1 < k < 0.4 \text{Mpc}^{-1}$  and the detection of  $10\Delta_{\text{HI}}^2$  will require more than 1000 hours of observation.

We finally consider the situation where all the available  $k$ -modes are combined for a detection of the HI 21-cm signal. Here we have a single parameter  $A_{\text{HI}}$  which is the amplitude of the HI 21-cm power spectrum. We have estimated the SNR for the measurement of  $A_{\text{HI}}$  using

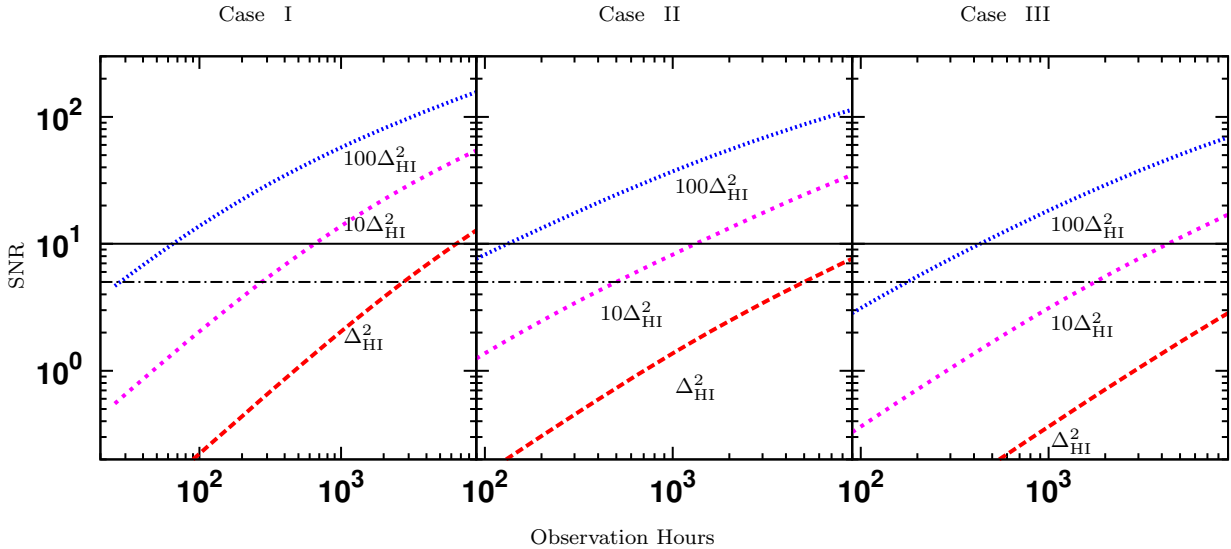
$$\text{SNR}^2 = \frac{1}{2} \sum_{\mathbf{k}_g} \left[ \frac{\partial P_{\text{HI}}(\mathbf{k}_g)}{\partial \ln A_{\text{HI}}} \right]^2 [P_{\text{HI}}(\mathbf{k}_g) + P_N(\mathbf{k}_g)]^{-2}. \quad (6)$$

Figure 2 shows the predicted SNR as a function of the observing time. The horizontal solid and the dot-dashed lines mark the SNR value of 10 and 5 respectively. For Case I we find that a  $10\sigma$  detection of  $100\Delta_{\text{HI}}^2$ ,  $10\Delta_{\text{HI}}^2$  and  $\Delta_{\text{HI}}^2$  is possible in  $\sim 70$ , 700 and 6000 hours of observation respectively. A  $5\sigma$  detection of  $\Delta_{\text{HI}}^2$  can be achieved in 3000 hours of observation. In Case II and Case III, it takes  $\sim 140$ , 1400 hours and  $\sim 400$ , 4000 hours for a  $10\sigma$  detection of  $100\Delta_{\text{HI}}^2$  and  $10\Delta_{\text{HI}}^2$  respectively. It is not possible to detect  $\Delta_{\text{HI}}^2$  within reasonable observation time when we consider the pessimistic scenario.

For comparison, we consider the upcoming SKA-Low which will operate within a frequency range of 50–350 MHz and investigate the prospects of detecting the redshifted HI 21-cm signal power spectrum from Cosmic Dawn. SKA-Low is expected to be an array of  $\sim 513$  stations, each



**Figure 1.** This shows a comparison of the dimensionless HI 21-cm signal power spectrum and the corresponding  $1 - \sigma$  error for an uGMRT observation. The left, middle and right panels show results for Case I, II and III respectively. The HI signal is shown in dashed lines (as mentioned in the figure). The error on the measurement of the power spectrum for 100, 500 and 1000 hours is shown in solid, dotted and fine-dotted lines respectively.



**Figure 2.** The left, middle and right panels show the predictions for Case I, II and III respectively when all the available  $k$ -modes are combined. The dashed, dotted and fine-dotted lines show the predictions for the HI 21-cm signal power spectrum  $\Delta_{\text{HI}}^2$ ,  $10\Delta_{\text{HI}}^2$  and  $100\Delta_{\text{HI}}^2$  respectively. The horizontal dot-dashed and solid lines mark the SNR of 5 and 10 respectively.

of diameter  $D = 35$  m. Modelling each station as having a circular aperture of diameter 35 m we estimate the primary beam pattern to have a full-width at half-maxima (FWHM) of  $6.44^\circ$ , and we model the primary beam pattern as a Gaussian  $A(\theta) = e^{-(\theta/\theta_0)^2}$  with  $\theta_0 = 0.62 \theta_{\text{FWHM}} = 4^\circ$  (Choudhuri et al. 2014). Using this we have calculated  $\tilde{\eta} = 39.44$  at the frequency of our interest. We have simulated the SKA-Low baseline distribution corresponding to 8 hrs of observation towards a fixed pointing direction at declination

$\delta = -30^\circ$ . We have used the proposed SKA-Low<sup>1</sup> antenna configuration for our simulation. The rest of the analysis was carried out along exactly the same lines as that for the uGMRT. Note that the grid spacing  $\Delta k_\perp$  was scaled appropriately to account for the different value of the diameter  $D$ , whereas the value of  $\Delta k_\parallel$  was maintained the same as for the uGMRT. Figure 3 shows a comparison between the dimensionless HI 21-cm signal power spectrum and the corresponding  $1 - \sigma$  error. For Case I we find that  $\Delta_{\text{HI}}^2$  can

<sup>1</sup> SKA1- LowConfigurationCoordinates-1.pdf

be detected with 100 hours of observation for Fourier modes  $0.02 < k < 1.0 \text{ Mpc}^{-1}$ . However, a detection of  $10\Delta_{\text{HI}}^2$  and  $100\Delta_{\text{HI}}^2$  will require less observation time. In Case II, it is possible to detect  $\Delta_{\text{HI}}^2$  in the  $k$ -range,  $0.1 < k < 1.0 \text{ Mpc}^{-1}$  and for the pessimistic scenario, *i.e.* Case III, we find that  $\Delta_{\text{HI}}^2$  can be detected in 100 hours of observation in the  $k$ -range  $0.2 < k < 1.0 \text{ Mpc}^{-1}$ . This results are significantly promising when compared to the uGMRT. It is a direct consequence of the fact that SKA-Low has larger number of antennas and better  $uv$ -coverage when compared to uGMRT. It is interesting to note that for SKA-Low the  $1-\sigma$  errors do not decrease very much as the observing time is increased from 100 to 1000 hrs, whereas we find a pretty significant decrease for uGMRT (Figure 1). This indicates that the  $1-\sigma$  errors for the SKA-Low are largely cosmic variance dominated whereas these are the system noise dominated for the uGMRT. Figure 4 shows the predicted SNR as a function of the observing time for SKA-Low. The horizontal solid and the dot-dashed lines mark the SNR value of 20 and 10 respectively. For Case I, II and III we find that a  $20\sigma$  detection  $\Delta_{\text{HI}}^2$  is possible in  $\sim 40, 60$  and  $200$  hours of observation respectively. Here again it is interesting to note that for SKA-Low the SNR does not increase as rapidly with the observing time as for the uGMRT (Figure 2). As noted earlier, this is a consequence of the fact that for SKA-Low the cosmic variance makes a larger contribution to the total error budget as compared to the uGMRT. Our predictions for SKA-Low are roughly consistent with the earlier predictions of Koopmans et al. (2015).

The upcoming experiment, the Hydrogen Epoch of Reionization Array (HERA; DeBoer et al. 2017) a 350-element interferometer is also expected to operate from 50 to 250 MHz. Note that HERA is a drift scan instrument unlike uGMRT and SKA-Low which can track a fixed pointing direction on the sky. Considering 1000 hrs of observation, at  $z = 17$  the HERA sensitivity is about 8 times better for the cosmic dawn HI 21-cm power spectrum measurement (DeBoer et al. 2017) as compared to uGMRT.

#### 4 CONCLUSION

If the proposed b-DM interaction (Barkana 2018; Fialkov et al. 2018) enhances the Cosmic Dawn HI 21-cm power spectrum, it can be detected with the Band-1 of uGMRT within reasonable hours of observation. Such a detection would be an independent confirmation of the enhanced dip reported by Bowman et al. (2018). The b-DM scattering model depends upon two additional parameters: the mass of the DM particles,  $0.0032 < m_\chi < 100 \text{ GeV}$  and the cross-section  $10^{-30} < \sigma_1 < 3.16 \times 10^{-18} \text{ cm}^2$ . This interaction model enhances the Cosmic Dawn HI 21-cm brightness temperature fluctuations and the maximal fluctuation amplitude (due to b-DM scattering only) is predicted to be between 0 and 850 mK, while the maximal fluctuation amplitude without b-DM scattering has been predicted to be anywhere between 1.5 and 90 mK (Fialkov et al. 2018). With the measurement of the Cosmic Dawn HI 21-cm power spectrum, one expects to constrain the  $m_\chi - \sigma_1$  parameter space. Observations with the Band-1 of uGMRT hold the prospect of being an interesting probe of the b-DM interaction in the early universe. Even upper limits from a

non-detection of this power spectrum would impose useful constraints on the mass of the DM particles, the scattering cross-section and the proposed b-DM interaction. We also note that the observations with the Band-1 of uGMRT hold the possibility to constraint the “minicharged” dark matter models. Even an upper limit from a non-detection of the the Cosmic Dawn HI 21-cm power spectrum can put an upper limit on such “minicharged” dark matter models. For example, considering 1000 hrs of observation with Case I, uGMRT would be sensitive enough to rule out models with the fraction of “minicharged” dark matter particles in the range  $f_{dm} \geq 0.03$  based on the HI 21-cm power spectrum predictions of Muñoz et al. (2018).

*Acknowledgement:* The authors would to thank Ravi Subrahmanyan for drawing their attention to the possibility of observing the Cosmic Dawn redshifted 21-cm signal using Band-1 of uGMRT. The authors would also like to thank Abinash K. Shaw and Anjan K. Sarkar for useful discussions. SC acknowledges the University Grants Commission, India for providing financial support through Senior Research Fellowship.

#### REFERENCES

- Ali S. S., Bharadwaj S., Chengalur J. N., 2008, MNRAS, 385, 2166
- Barkana R., 2018, Nature, 555, 7694, 71
- Bernardi G., Zwart J. T. L., Price D., et al., 2016, Monthly Notices of the Royal Astronomical Society, 461, 3, 2847
- Bharadwaj S., Ali S. S., 2005, MNRAS, 356, 1519
- Bowman J. D., Rogers A. E. E., Monsalve R. A., Mozdzen T. J., Mahesh N., 2018, Nature, 555, 7694, 67
- Chengalur J. N., Gupta Y., Dwarkanath K., 2007, Low frequency radio astronomy 3rd edition
- Choudhuri S., Bharadwaj S., Ghosh A., Ali S. S., 2014, MNRAS, 445, 4351
- Cohen A., Fialkov A., Barkana R., Lotem M., 2017, Monthly Notices of the Royal Astronomical Society, 472, 2, 1915
- Datta A., Bowman J. D., Carilli C. L., 2010, ApJ, 724, 526
- DeBoer D. R., Parsons A. R., Aguirre J. E., et al., 2017, Publications of the Astronomical Society of the Pacific, 129, 974, 045001
- Dvorkin C., Blum K., Kamionkowski M., 2014, Phys. Rev. D, 89, 023519
- Ewall-Wice A., Chang T. C., Lazio J., Dore O., Seiffert M., Monsalve R. A., 2018, arXiv:1803.01815
- Feng C., Holder G., 2018, The Astrophysical Journal Letters, 858, 2, L17
- Fialkov A., Barkana R., Cohen A., 2018, arXiv:1802.10577
- Gupta Y., Ajithkumar B., Kale H., et al., 2017, CURRENT SCIENCE, 113, 4, 707
- Koopmans L. V. E., et al., 2015, PoS, AASKA14, 001
- Mellema G., Koopmans L. V. E., Abdalla F. A., et al., 2013, Experimental Astronomy, 36, 1, 235
- Morales M. F., Hazelton B., Sullivan I., Beardsley A., 2012, ApJ, 752, 137
- Muñoz J. B., Dvorkin C., Loeb A., 2018, arXiv:1804.01092
- Muñoz J. B., Kovetz E. D., Ali-Haïmoud Y., 2015, Phys. Rev. D, 92, 083528
- Muñoz J. B., Loeb A., 2018, Nature, 557, 7707, 684
- Parsons A. R., Pober J. C., Aguirre J. E., Carilli C. L., Jacobs D. C., Moore D. F., 2012, ApJ, 756, 165
- Philip L., Abdurashidova Z., Chiang H. C., et al., 2018, arXiv:1806.09531
- Pober J. C., Liu A., Dillon J. S., et al., 2014, ApJ, 782, 66

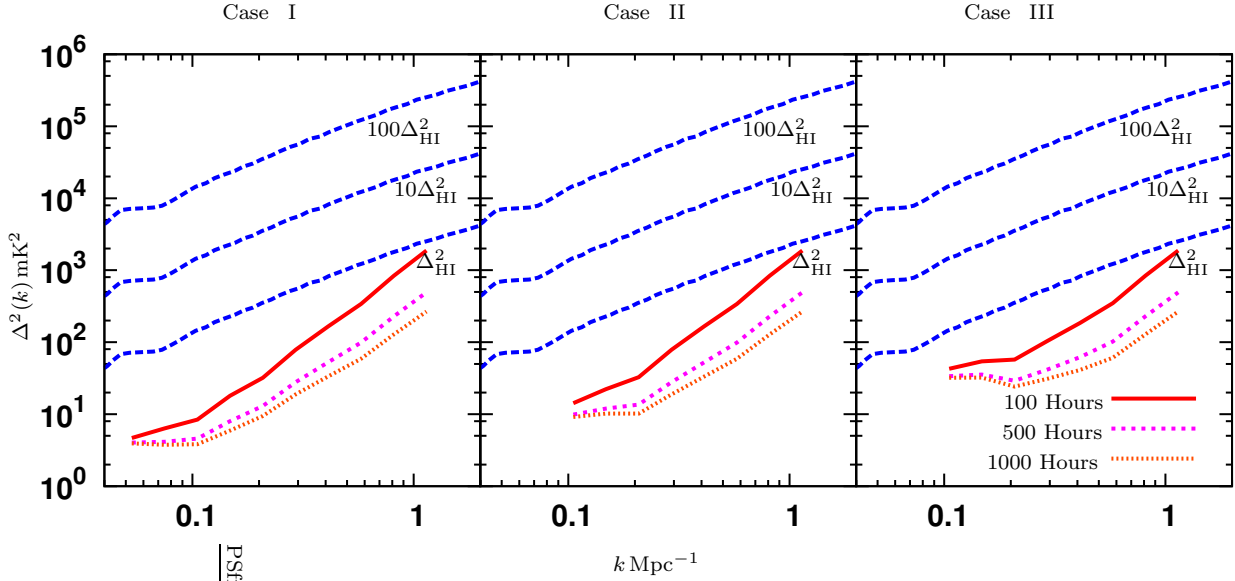


**Figure 3.** This shows a comparison of the dimensionless HI 21-cm signal power spectrum and the corresponding  $1 - \sigma$  error for an SKA-Low observation. The left, middle and right panels show results for Case I, II and III respectively. The HI signal is shown in dashed lines (as mentioned in the figure). The error on the measurement of the power spectrum for 100, 500 and 1000 hours is shown in solid, dotted and fine-dotted lines respectively.

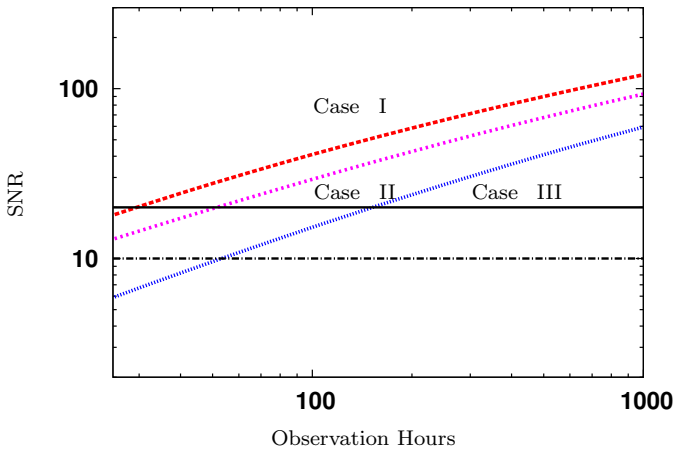


**Figure 4.** The dashed, dotted and fine-dotted lines show the predictions for Case I, II and III respectively when all the available  $k$ -modes are combined. The horizontal dot-dashed and solid lines mark the SNR of 10 and 20 respectively.

- Trott C. M., Wayth R. B., Tingay S. J., 2012, *The Astrophysical Journal*, 757, 1, 101  
 Vedantham H., Udaya Shankar N., Subrahmanyan R., 2012, *ApJ*, 745, 176  
 Voytek T. C., Natarajan A., García J. M. J., Peterson J. B., López-Cruz O., 2014, *The Astrophysical Journal Letters*, 782, 1, L9  
 Xu W. L., Dvorkin C., Chael A., 2018, *Phys. Rev. D*, 97, 103530

- Pritchard J. R., Loeb A., 2012, *Reports on Progress in Physics*, 75, 8, 086901  
 Santos M. G., Ferramacho L., Silva M. B., Amblard A., Cooray A., 2010, *Monthly Notices of the Royal Astronomical Society*, 406, 4, 2421  
 Shankar N. U., Dwarakanath K., Amiri S., et al., 2009, *The Low-Frequency Radio Universe*, 407, 393  
 Singh S., Subrahmanyan R., Shankar N. U., et al., 2017, *The Astrophysical Journal Letters*, 845, 2, L12  
 Swarup G., Ananthakrishnan S., Kapahi V. K., Rao A. P., Subrahmanya C. R., Kulkarni V. K., 1991, *Current Science*, Vol. 60, NO.2/JAN25, P. 95, 1991, 60, 95  
 Tashiro H., Kadota K., Silk J., 2014, *Phys. Rev. D*, 90, 083522